

Reactive Oxygen-induced Carcinogenesis Causes Hypermethylation of *p16^{Ink4a}* and Activation of MAP Kinase

Baskaran Govindarajan,¹ Robert Klafter,² Mark Steven Miller,³ Claire Mansur,⁴ Melissa Mizesko,³ Xianhe Bai,¹ Kenneth LaMontagne Jr,⁵ and Jack L Arbiser¹

¹Department of Medicine, Dermatology

²Department of Medicine, Hematology/Oncology, Emory University School of Medicine, Atlanta, GA, USA

³Department of Cancer Biology, Comprehensive Cancer Center, Wake Forest University School of Medicine, Winston-Salem, NC, USA

⁴Department of Dermatology, Tufts University School of Medicine

⁵Department of Surgical Research, Children's Hospital-Harvard Medical School, Boston, MA, USA

Communicated by J. Folkman. Accepted January 15, 2002

Abstract

Background: Implantation of foreign materials into mice and humans has been noted to result in the appearance of soft tissue sarcomas at the site of implantation. These materials include metal replacement joints and Dacron vascular grafts. In addition, occupational exposure to nickel has been shown to result in an increased risk of carcinogenesis. The molecular mechanisms of foreign body-induced carcinogenesis are not fully understood.

Materials and Methods: In order to gain insight into these mechanisms, we implanted nickel sulfide into wild type C57BL/6 mice as well as a mouse heterozygous for the tumor suppressor gene, *p53*. Malignant fibrous histiocytomas arose in all mice, and we have characterized the

profile of tumor suppressor genes and signal transduction pathways altered in these cells.

Results: All tumors demonstrated hypermethylation of the tumor suppressor gene *p16*, as well as activation of the mitogen activated protein kinase (MAP kinase) signaling pathway. This knowledge may be beneficial in the prevention and treatment of tumors caused by foreign body implantation.

Conclusions: Oxidative stress induced by nickel sulfide appears to cause loss of *p16* and activation of MAP kinase signaling. These findings support the hypothesis of synergistic interactions between MAP kinase activation and *p16* loss in carcinogenesis.

Introduction

Oxidative stress is thought to be a major contributor to multiple forms of carcinogenesis, including chemical-, ultraviolet-, and radiation-induced cancers (1–4). The precise mechanisms of oxidative stress-induced carcinogenesis are not fully elucidated. In order to gain insight into these mechanisms, we used the nickel sulfide model of oxidative carcinogenesis. Nickel sulfide is an insoluble carcinogen which is thought to act through the production of free radicals (5–8). Phagocytosis and solubilization of nickel sulfide have been established as necessary steps in the generation of nickel-induced tumors (9,10). Both soluble and insoluble forms of nickel have been implicated in human cancer, with the generation of soluble Ni²⁺ thought to be a common factor (11). While insoluble nickel has been associated with the development of soft tissue sarcomas, soluble nickel has been associated with the

development of epithelial malignancies and has been shown to induce immortalization of human kidney epithelium (12,13). Regulation of several genes by nickel has been demonstrated, including Cap43, acetylation of histone H4, and HIF-1 transcription factor (14–16).

We implanted nickel sulfide intramuscularly into wild-type C57BL/6 mice and into a mouse heterozygous for *p53*. Sarcomas arose at the site of implantation with a latency of approximately eight months in the wild type mice, and at three months in a mouse heterozygous for *p53*. Primary tumor tissue and cell lines derived from these sarcomas were analyzed for inactivation of tumor suppressor genes and activation of signal transduction pathways. All tumors demonstrated hypermethylation of the promoter of the *p16^{Ink4a}* gene. Expression of the alternate reading frame of the *Ink4a* locus, *p19^{ARF}*, was observed in tumor-derived cells. Cell lines derived from these tumors also showed high level MAP kinase activation. These results show that nickel sulfide-induced tumorigenesis leads to activation of the MAP kinase signaling pathway and loss of expression of tumor suppressor genes.

Address correspondence and reprint requests to: Jack L Arbiser, Department of Dermatology, Emory University School of Medicine, 1639 Pierce Drive, WMB 5309, Atlanta, GA, 30322, Tel (404) 727-5063; fax (404) 727-5878; e-mail jarbise@emory.edu.

Materials and Methods

Development of Tumors and Tumor-derived Cell Lines

Five mg of nickel sulfide (Ni_3S_2 , 150 mesh, Aldrich Chemical Company catalog number 343226) were suspended in 0.3 ml of DMEM supplemented with 10% fetal calf serum, and the suspension was injected into the right rear legs of three wild type C57BL6 mice (Jackson Laboratories, Bar Harbor Maine) and a p53 +/- mouse (C57BL6 background, Genpharm, Mountain View, CA). As a control, 0.3 ml of tissue culture media without nickel sulfide was injected into the left rear leg of the same mice. After eight months, tumors were present in the right limb of the wild-type mice, and after three months in the p53 heterozygous mouse. No tumors were visible in the left limb of any mice. Tumors were explanted into tissue culture, consisting of Dulbeccos Modified Eagle Medium (DMEM) supplemented with 5% fetal calf serum and penicillin/streptomycin. The resulting tumors and cell lines were named C57NiS1-3 in the case of tumors derived from wild-type mice, and p53NiS1 in the case of the tumor derived from the p53 heterozygote mouse, because the tumors were induced by nickel sulfide (NiS). Tumors were used for the genetic analysis of the wild type mice, and early passage cell lines derived from the tumors were used for the signal transduction analysis. We analyzed tumors for the genetic mutations as we did not want to examine mutations that may have occurred outside of the mouse. Similarly, we examined early passage cells from tumor for signal transduction events in order to avoid contamination by growth factor-activated stromal cells, i.e., angiogenic endothelium, which might cause a false positive result (17).

Electron Microscopy

Cell pellets were immersed in 4% cacodylate-buffered glutaraldehyde. After fixation, the cells were washed in buffer, fixed in 1% OsO_4 solution, dehydrated in graded ethanols and propylene oxide, and embedded in Embed-812 epoxy resin (Electron Microscopy Sciences, Fort Washington, PA). Thick sections (0.5 μM) cut with glass knives were stained with Toluidine Blue. Ultrathin sections (0.1 μM) were cut with a diamond knife and mounted on 200 mesh copper grids, stained with uranyl acetate and lead citrate, and photographed with a Phillips EM201 electron microscope.

Signal Transduction Analysis

Three million cells were lysed in 1 ml lysis buffer containing 20 mM Tris HCl (pH 7.5), 150 mM NaCl, 1% (v/v) Triton X-100, 10% glycerol, 1 mM EDTA, 10 $\mu\text{g}/\text{ml}$ leupeptin, 10 $\mu\text{g}/\text{ml}$ aprotinin, 1 mM benzamide, 1 mM phenylmethylsulfonyl fluoride, and 1 mM Na_3VO_4 . The lysate was spun in a microfuge, and the pellet was discarded. Protein concentration of the supernatant was determined by the Bradford

assay using BSA as a standard. Samples were treated with Laemmli sample buffer and heated to 90°C for 5 minutes prior to SDS-PAGE (National Diagnostics, Atlanta, GA) and transferred to nitrocellulose membranes. The membranes were then blocked with 5% nonfat dry milk in 10 mM Tris/0.1% Tween 20/100 mM NaCl and subsequently incubated with the appropriate antibody for immunoblotting. Anti phospho-AKT polyclonal antibody and anti phospho-MAPK polyclonal antibody were obtained from New England Biolabs, (Beverly, MA). Western blotting was performed according to Arbiser et al (18). Cell lines rather than tumor tissue were examined for signal transduction analysis to avoid potential stromal contamination, which might confound the analysis (17).

PCR Amplification and Gene Sequence Analysis

One to 2 μg of DNA from tumor tissue in the case of wild-type tumors, or an equivalent quantity from early passage p53NiS1 cells were amplified using the Perkin-Elmer GeneAmp PCR Reagent Kit. All reactions were carried out in a 50 μl reaction volume, which consisted of buffer (10 M Tris-HCl, pH 8.0/50 mM KCl), 2.5 mM MgCl_2 (concentration adjusted to 4.0 mM for exon 8 p53), 200 μM dNTPs (dATP, dCTP, dGTP, dTTP), and 2 units of AmpliTaq Gold (Perkin-Elmer Cetus, Norwalk, CT). Primers for the Ki-ras, p53, (Oligos Etc, Guilford, CT), p16^{Ink4a}, and p19^{ARF} genes (DNA Synthesis Core Laboratory, Comprehensive Cancer Center, Wake Forest University) were added at a final concentration of 0.2 μM for each primer as described previously (19–21). Intronic primers were used for p53 because of the presence of pseudogenes in the mouse genome (22). The samples were overlaid with 50 μl of mineral oil to prevent evaporation and cross contamination of the samples. All PCR reaction conditions started with an initial extended denaturation step for 4 minutes at 94°C and ended with a prolonged extension step for 5–7 minutes at 72°C. Gene-specific amplification for 30–40 cycles was as follows: exon 1 of the Ki-ras gene, 1 min at 94°C, 1 min at 50°C and 1 min at 72°C; exons 1 α and 2 of p16^{Ink4a} and exon 2 of Ki-ras, 1 min at 94°C, 1 min at 58°C, and 1 min at 72°C; exon 1 β of p19^{ARF}, 1 min at 94°C, 1 min at 67°C and 1 min at 72°C (19–21); exon 5–8 of p53, 1 minute at 94°C and 2 minutes at 65°C (21,23). Each reaction included negative controls, which lacked template DNA and served as negative buffer controls for the PCR amplification reactions. All samples were amplified in an Ericomp DeltaCycler II System.

Following amplification, the samples were electrophoresed on a 3% Nu-Sieve gel (FMC Bio-products, Rockland, ME) to visualize the PCR products. The PCR products were then either gel purified or taken directly from the PCR mix, purified with the QiaQuick PCR Purification Kit (Qiagen Inc., Chatsworth, CA), and the sequences determined by direct automated DNA sequencing using the ABI

PRISM Dye Terminator Cycle Sequencing Ready Reaction Kit (Perkin-Elmer, Foster City, CA) according to the manufacturer's instructions. Analysis of the DNA sequences was done using the DNASIS software (Hitachi Software Engineering America, Ltd., San Bruno, CA).

Methylation-Specific PCR

Methylation-specific PCR was performed by the method of Herman et al. (24,25) using the following primers: methylated DNA, forward primer 5'-AATTCGAGGAGAGTTATTTG-3', reverse primer 5'-AAATCGAAATACGACCGAAA-3'; unmethylated DNA, forward primer 5'-AATTTGAGGAGAGTTATTTG-3', reverse primer 5'-AAATCAAATACAA-CCAAAAA-3'. DNA was denatured by addition of NaOH to a final concentration of 0.2 M and incubation for 10 minutes at 37°C. Freshly prepared sodium bisulphite and hydroquinone were added as part of modification reagent I of the CpGenome Modification Kit (Oncor, Gaithersburg, MD) and incubated at 50°C overnight. Modified DNA was subsequently column purified using the *Promega Wizard DNA Clean-up Kit*. NaOH was added to a final concentration of 0.3 M, the samples incubated at room temperature for 5 minutes, and the DNA removed by ethanol precipitation. The modified DNA was amplified by PCR as described above. Following an initial denaturation at 95°C for 10 minutes, the DNA was amplified with methylation specific primers for 40 cycles of 95°C for 1 minute, 52°C for 1 minute, and 72°C for 1 minute, followed by a final extension of 72°C for 7 minutes. PCR products were visualized on a 3% Agar H/S gel (Continental Laboratory Products, San Diego CA). Methylated CpG residues will be resistant to deamination following treatment with bisulphite, while unmethylated cytosines will

be converted to uracil, resulting in a C to T transition in the PCR products at unmethylated CpG sites.

Results

Inoculation of nickel sulfide into the thigh muscle of both wild type and p53 heterozygous mice lead to development of sarcomas (Fig. 1). Histologically and ultrastructurally, the tumor cells resembled malignant fibrous histiocytomas (Fig. 2A, B). Cell lines derived from these tumors were analyzed for the activation of the MAP kinase and phosphoinositol-3 kinase (PI-3 K) pathways through Western analysis of cell lysates with antibodies specific for phospho-specific MAP kinase and phospho-specific Akt, respectively (26). Extremely high levels of phosphorylated MAP kinase were observed, indicating high level activation of this pathway (Fig. 3). Lower levels of phospho-Akt were observed, indicating modest activation of the PI-3 K pathway (data not shown). We are unable to compare the levels of activation of MAP kinase and PI-3 K between p53NiS1 cells and their precursors, because the cell of origin in our study is unknown. However, the levels of activation in p53NiS1 cells are elevated compared with historical controls, i.e., MS1 cells, a nontumorigenic endothelial cell line derived from introduction of SV40 large T antigen into endothelial cells (Fig. 3) (18). Similarly high levels of phosphorylated MAP kinase and akt were observed in cells from wild-type tumors.

To determine if tumor tissue and the tumor-derived cell line contained structural alterations (such as point mutations, deletions, or additions) at oncogenic loci, we amplified and sequenced 4 genetic loci that have been frequently implicated in human carcinogenesis. Our results show that exons 1 α , 1 β and 2 from the *Ink4a* locus (coding for the two gene

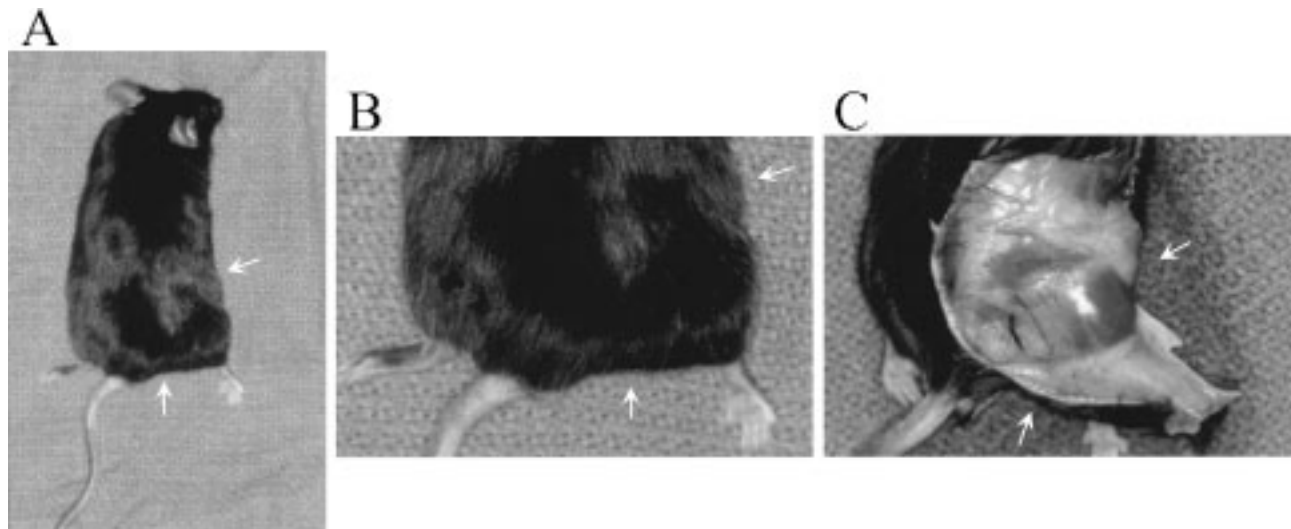


Fig. 1. Gross view of nickel-sulfide induced sarcoma arising in a mouse. Limb asymmetry in site of sarcoma (arrows) (1A), closeup of tumor (1B), and appearance of sarcoma under the skin (1C).

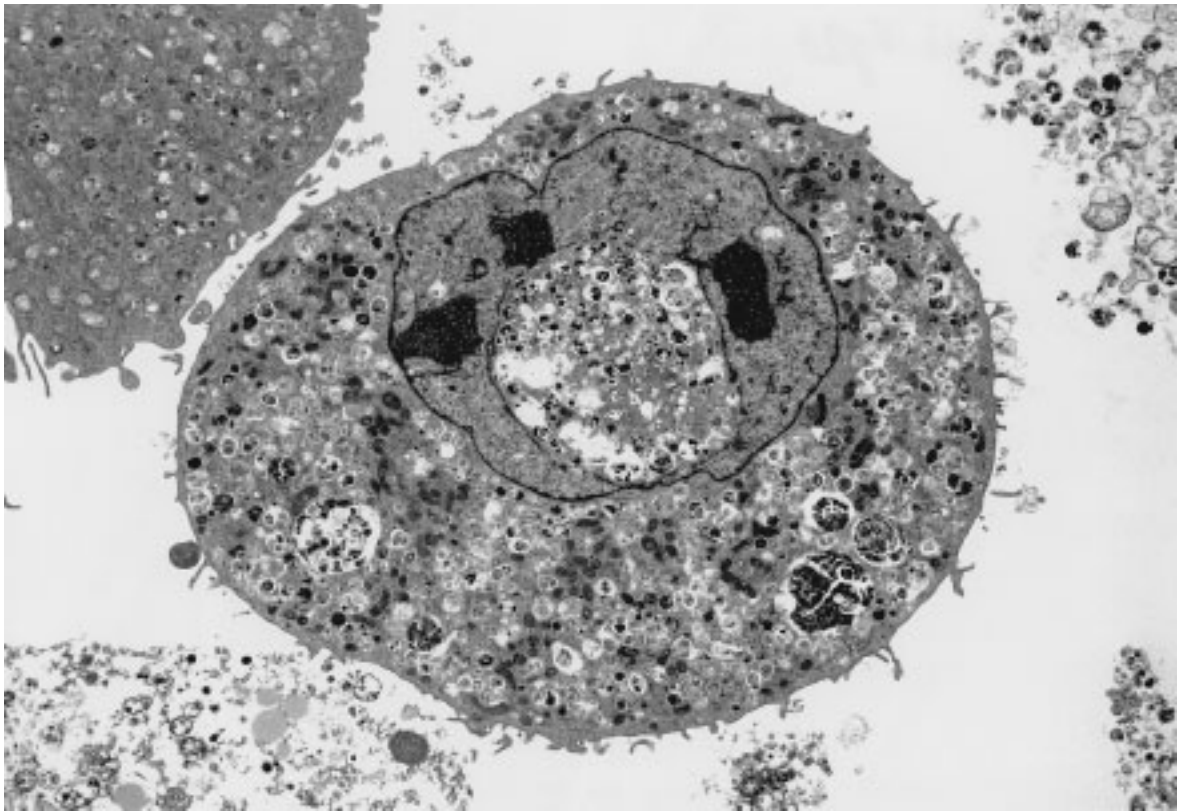
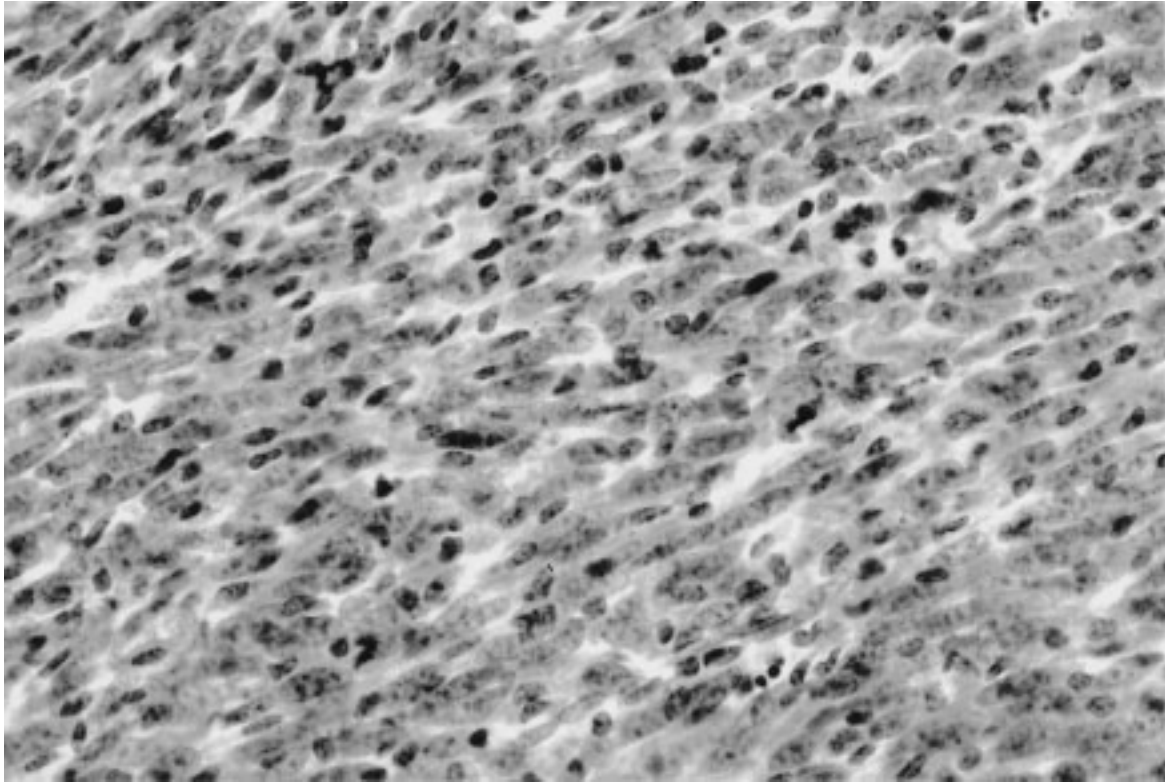


Fig. 2. Tumor histology and ultrastructure of p53NiS1 cells. Histologic appearance of original tumor generated by injection of NiS in p53 +/- mouse at 40X magnification (2A) and ultrastructural appearance of p53NiS1 cells showing abundant lysosomes, characteristic of malignant fibrous histiocytoma (5000x) (2B).

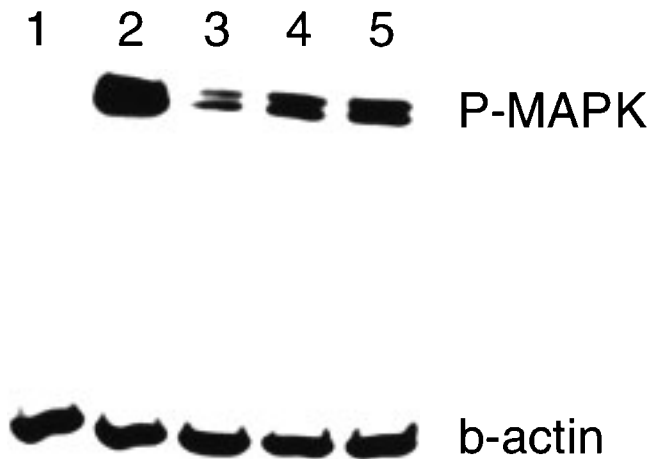


Fig. 3. Western blot analysis of cell lines derived from nickel sulfide induced malignant fibrous histiocytomas showing expression of phosphorylated MAP kinase with β -actin as a loading control. Levels of phosphorylation are compared with MS1 (lane 1). P53Nis1 cell lysates are in lane 2, and C57Nis1,2,3 are in lanes 3,4, and 5 respectively.

products associated with the *Ink4a* locus, $p16^{Ink4a}$ and $p19^{ARF}$) contained normal, wild-type sequences. One tumor expressed a potentially oncogenic mutation in *Ki-ras* (Table 1). In addition, exons 6, 7, and 8 of *p53* also exhibited normal sequences in all tumors and cells examined. Interestingly, we were unable to amplify exon 5 of *p53* using the same intronic primers utilized in previous studies (21). This suggested that either there was a small mutation in the sequence that prevented binding of one of the primers, or a portion of the gene was deleted. To distinguish between these two possibilities, we used a different set of primer sequences.

The 5' forward primer used to amplify exon 5 sequences was located in intron 4 while the 3' primer was located at the juncture between intron 5 and exon 6. We subsequently synthesized an exonic primer that was complementary to the first 21 bases of exon 5, approximately 30 bp downstream of the original primer site. This was paired with the 3' primer used to amplify exon 6. A multiplex reaction was then set up that included this new 5' primer and the 3' primer to intron 6 as well as amplimers to

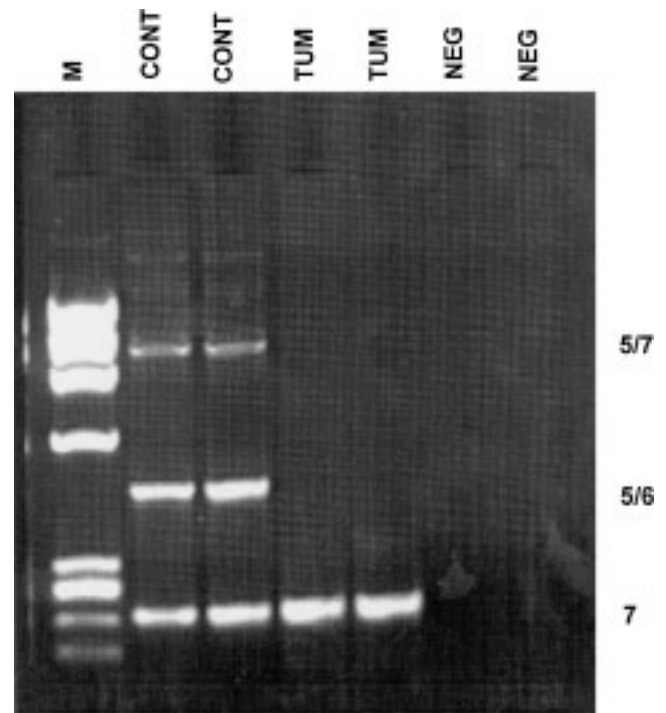


Fig. 4. PCR amplification of exon 5 of the *p53* gene. One to 2 μ g of DNA isolated from normal mouse lung (CONT) tissue and the tumor cell line (TUM) were amplified in a multiplex reaction mixture containing primers that yield a 49 bp fragment from exon 5 to intron 6 (5/6) and a 234 bp fragment for exon 7 sequences spanning intron 6 to intron 7. Only the CONT samples showed amplification of both PCR fragments, suggesting the presence of a deletion in the *p53* allele in the transgenic mice from which the tumor was derived. A higher molecular weight fragment spanning sequences from exon 5 to intron 7 is also visible in the CONT samples (5/7). The lanes marked "NEG" were negative controls that lacked any added DNA; lane marked "M" contains molecular weight markers.

exon 7 as a positive control for amplification. DNA isolated from the normal lung of a C57BL/6 mouse (Fig. 4) produced the anticipated 3 PCR products: a 234 bp product for exon 7, a 449 bp product spanning exon 5, intron 5, exon 6 and part of intron 6, and a larger product (>700 bp) that was the result of amplification from exon 5 through intron 7. Only the exon 7 product was visible in DNA isolated from the tumor cell line, suggesting the presence of a deletion

Table 1. Spectrum of mutations in nickel sulfide-induced sarcomas

Tumor	p16	p53	H and K-ras
P53NiS1	hypermethylation	deletion exon 5	none
C57NiS1	hypermethylation	A to C mutation in Intron 7 of p53	none
C57NiS2	hypermethylation	none	G to A in codon 12 of <i>Ki-ras</i> No <i>H-ras</i> mutations
C57NiS3	hypermethylation	none	none

of at least 35 base pairs in the 5' region of exon 5, possibly including the 3' region of intron 4 (Fig. 4). In tumor tissue derived from wild-type mice, *p53* mutation did not appear to be a consistent feature, as two of the tumors exhibited no alteration while one tumor exhibited a point mutation, an A to C transversion at the next to the last base of an intron (Table 1). This could be a potential splice site and thus could potentially interrupt normal gene expression.

Several studies have suggested that *Ink4a* can be transcriptionally silenced by promoter hypermethylation rather than mutation or other structural alterations. We explored this possibility by using the bisulfite modification procedure coupled with MS-PCR as described by Herman et al (24). In this reaction, all unmethylated cytosines are deaminated and converted to uracils by the bisulfite reaction. Methylated CpG residues are protected. Thus, upon amplification, the sequences will differ in these regions depending on whether the CpG residues are methylated or not. Two different primer sets were used that could distinguish between these different sequences in exon 1 α of the *Ink4a* locus (25). Normal genomic mouse DNA (purchased from Clontech) produced a PCR product only with primers specific for unmethylated CpG residues (Fig. 5). In contrast,

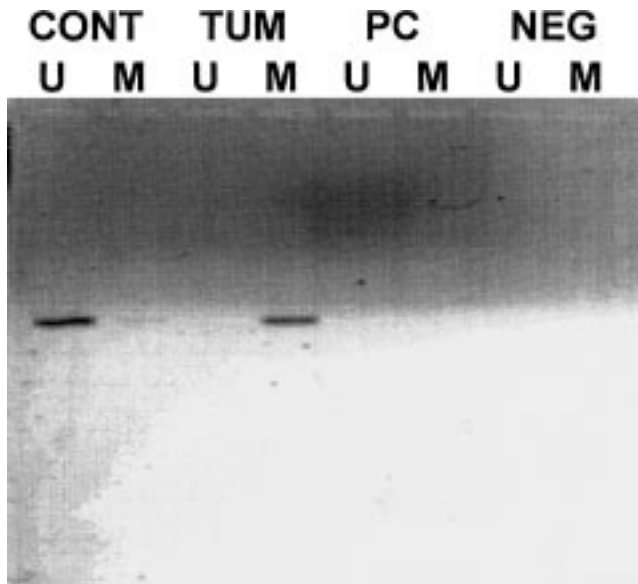


Fig. 5. Methylation-specific PCR of exon 1 α of the *p16^{Ink4a}* gene. One to 2 μ g of normal mouse DNA purchased from Clontech (CONT) and tumor cell DNA (TUM) were modified by treatment with bisulfite and subjected to PCR with primers specific for either methylated (M primers) or unmethylated (U primers) CpG residues. CONT DNA exhibited a PCR product only with primers specific for unmethylated DNA while the tumor cell DNA only yielded a PCR product with the primers specific for methylated DNA. The lanes marked PC were procedure controls that lacked any added DNA and were taken through all of the experimental steps; lanes marked NEG were negative buffer controls for the PCR reaction and also lacked any added DNA template. Similar results were observed in DNA derived from wild-type tumors.

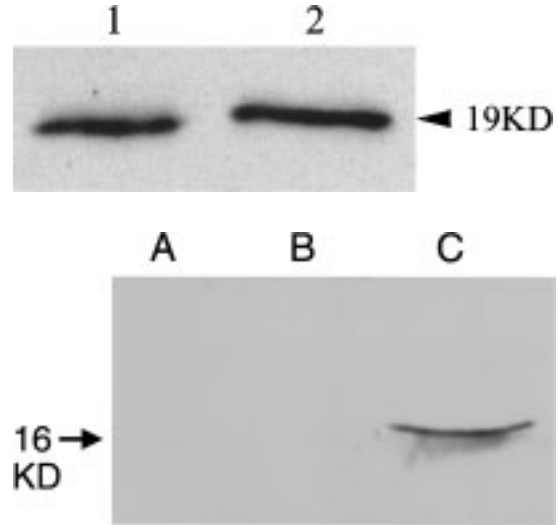


Fig. 6. Western blot analysis of p53NiS1 cells showing expression of *p19^{ARF}* and lack of expression of *p16*. In this Western blot analysis of *p19^{ARF}* (6A), the left lane contains lysate from SVR cells, and the right lane contains lysate from p53NiS1 cells. In this Western blot analysis of *p16* expression (6B), lane A contains whole cell lysate of p53NiS1 cells, lane B contains RIPA lysate of p53NiS1 cells, and lane C contains 3T3 L1 cells as a positive control.

DNA from p53NiS1 only amplified with the primers specific for methylated CpG sequences, suggesting that *p16^{Ink4a}* has been transcriptionally silenced in these cells by promoter hypermethylation.

Interestingly, hypermethylation of the *p16^{Ink4a}* promoter was observed in all three primary tumor tissues derived from the wild type mice, in addition to the p53NiS1 cell line, suggesting that hypermethylation may be a common feature of nickel-sulfide induced carcinogenesis (Table 1, Fig. 5). The alternative gene product for this gene, *p19^{ARF}*, was evaluated for protein expression by Western blot analysis of p53NiS1. This cell line did express *p19^{ARF}* protein, while *p16^{Ink4a}* was not detectable by Western blot, as anticipated (Fig. 6). Thus, nickel sulfide is capable of causing a spectrum of mutations, but only *p16^{Ink4a}* hypermethylation and MAP kinase activation appear to be a common feature of nickel sulfide carcinogenesis.

Discussion

Particulate nickel sulfide is a well-established model of chemical carcinogenesis, and is thought to occur through a process of phagocytosis, solubilization of insoluble nickel, and resulting genetic changes (5,15,27). Mining and smelting of nickel is thought to contribute to carcinogenesis in humans, and nickel sulfide occurs naturally as the mineral millerite (28,29). In addition, sarcomas are observed at an increased frequency next to metal prostheses and Dacron grafts, and these tumors often exhibit phagocytic capabilities (malignant fibrous histiocytomas) (30–32). Thus, nickel may serve as a carcinogen in mice and humans.

Nickel treatment of cells has both acute and chronic effects. Among these is induction of oxidative stress (33,34). Nickel is chemically similar to cobalt, and acutely can stimulate genes that are also inducible by cobalt. These genes are regulated by the transcription factor hypoxia inducible factor-1 (HIF-1 α) and cobalt and nickel treatment is used experimentally to mimic hypoxia (35). Chronically, genetic changes have been observed, including immortalization of human kidney epithelium and methylation of the angiogenesis inhibitor thrombospondin-1 (13,36). However, the effect of chronic nickel exposure on tumor suppressor genes and signal transduction pathways is not fully understood.

We generated malignant fibrous histiocytomas through the injection of insoluble nickel sulfide intramuscularly into wild-type mice and a mouse heterozygous for the tumor suppressor gene *p53*. Tumor tissues and cell lines derived from these tumors were examined for alterations in the tumor suppressor genes *p53* and *p16^{Ink4a}*, as well as the dominant oncogenes *H-* and *Ki-ras*. The promoter region of *p16^{Ink4a}* exon 1 α was methylated in primary tumor tissue from all wild type mice and the p53NiS1 cell line, suggesting that hypermethylation of *p16^{Ink4a}* is a common feature of nickel sulfide-induced carcinogenesis. Similarly, high levels of activation of the MAP kinase pathway appear to be a common feature of nickel sulfide induced carcinogenesis.

Loss of p16 appears to be a common mechanism of tumorigenesis in a variety of genetic and environmentally induced cancers. Examples of human tumors which commonly demonstrate loss of *p16^{Ink4a}* expression include melanoma, oral squamous cell carcinoma, bladder cancer, and pancreatic carcinoma (37,38). The role of MAP kinase activation in these tumors has not been extensively studied, but constitutively activated MAP kinase is capable of transforming NIH3T3 cells (39,40), a cell line known to be deficient in *p16^{Ink4a}* (41–45).

Our data suggest that nickel sulfide-induced mutagenesis may result in inactivation of the tumor suppressor gene *p16^{Ink4a}* and activation of MAP kinase signaling. We have recently noted the common confluence of deletion of this tumor suppressor gene with activation of MAP kinase signaling (46). Of interest, we note hypermethylation of *p16^{Ink4a}* as a common event in the tumors and a cell line derived from nickel sulfide induced carcinogenesis. This is analogous to what is observed in environmentally induced carcinomas, such as cutaneous melanomas, which have *p16^{Ink4a}* inactivation in a vast majority of tumors, but may have various secondary hits required to cause full malignancy (47). Our results imply that a given carcinogen may cause repression of a specific tumor suppressor gene, such as *p16^{Ink4a}*, but may activate a variety of secondary events to cause transformation. This knowledge may be beneficial in the prevention and treatment of foreign-body induced tumors.

Acknowledgments

This project was funded by a Dermatology Foundation Dermik Laboratories Research Grant, a grant from the American Skin Association, grants from the National Institutes of Health AR02030 and RO1 AR47901, and NIAMS Emory Skin Disease Research Core Center P30 AR42687 (JLA). We acknowledge Drs. Lynda Chin and Jef French for helpful discussion. This project was supported in part by the National Research Service Award (NRSA), HL07842 (RK) from the National Institutes of Health, National Heart, Lung and Blood Institute, grants RO1 ES06501 and ES08252 (MSM) from the National Institute of Environmental Health Sciences and Cancer Center Support Grant P30 CA12197 from the National Cancer Institute, which provided support for the Wake Forest University Analytical Imaging Core Facility, the DNA Synthesis Core Laboratory, and the DNA Sequencing and Gene Analysis Facility. We thank Ms. Elyse Jung for assistance with the automated sequencing. Presented in part at the American Association for Cancer Research 91st Annual Meeting, San Francisco, 2000.

References

1. Lotem J, Peled-Kamar M, Groner Y, Sachs L. (1996) Cellular oxidative stress and the control of apoptosis by wild-type p53, cytotoxic compounds, and cytokines. *Proc. Natl. Acad. Sci. USA* **93**: 9166–9171.
2. Driscoll KE, Carter JM, Howard BW, et al. (1998) Crocidolite activates NF-kappa B and MIP-2 gene expression in rat alveolar epithelial cells. Role of mitochondrial-derived oxidants. *Environ. Health Perspect.* **106** Suppl 5: 1171–1174.
3. Meyskens FL, Jr, Buckmeier JA, McNulty SE, Tohidian NB. (1999) Activation of nuclear factor-kappa B in human metastatic melanomacells and the effect of oxidative stress. *Clin. Cancer Res.* **5**: 1197–1202.
4. Tanaka T, Iwasa Y, Kondo S, et al. (1999) High incidence of allelic loss on chromosome 5 and inactivation of p15INK4B and p16INK4A tumor suppressor genes in oxystress-induced renal cell carcinoma of rats. *Oncogene* **18**: 3793–3797.
5. Costa M, Mollenhauer HH. (1980) Phagocytosis of nickel subsulfide particles during the early stages of neoplastic transformation in tissue culture. *Cancer Res.* **40**: 2688–2694.
6. Costa M. (1991) Molecular mechanisms of nickel carcinogenesis. *Annu. Rev. Pharmacol. Toxicol.* **31**: 321–337.
7. Klein CB, Costa M. (1997) DNA methylation, heterochromatin and epigenetic carcinogens. *Mutat. Res.* **386**: 163–180.
8. Nackerdien Z, Kasprzak KS, Rao G, et al. (1991) Nickel(II)- and cobalt(II)-dependent damage by hydrogen peroxide to the DNA bases in isolated human chromatin. *Cancer Res.* **51**: 5837–5842.
9. Abbracchio MP, Heck JD, Costa M. (1982). The phagocytosis and transforming activity of crystalline metal sulfide particles are related to their negative surface charge. *Carcinogenesis* **3**: 175–180.
10. Costa M, Abbracchio MP, Simmons-Hansen J. (1981) Factors influencing the phagocytosis, neoplastic transformation, and cytotoxicity of particulate nickel compounds in tissue culture systems. *Toxicol. Appl. Pharmacol.* **60**: 313–323.
11. Abbracchio MP, Simmons-Hansen J, Costa M. (1982) Cytoplasmic dissolution of phagocytized crystalline nickel sulfide particles: a prerequisite for nuclear uptake of nickel. *J. Toxicol. Environ. Health* **9**: 663–676.
12. Reger RB, Morgan WK. (1993) Respiratory cancers in mining. *Occup. Med.* **8**: 185–204.

13. Tveito G, Hansteen IL, Dalen H, Haugen A. (1989) immortalization of normal human kidney epithelial cells by nickel(II). *Cancer Res.* **49**: 1829–1835.
14. Broday L, Peng W, Kuo MH, et al. (2000) Nickel compounds are novel inhibitors of histone H4 acetylation. *Cancer Res.* **60**: 238–241.
15. Salnikow K, Blagosklonny MV, Ryan H, et al. (2000) Carcinogenic nickel induces genes involved with hypoxic stress. *Cancer Res.* **60**: 38–41.
16. Salnikow K, Kluz T, Costa M. (1999) Role of Ca(2+) in the regulation of nickel-inducible Cap43 gene expression. *Toxicol. Appl. Pharmacol.* **160**: 127–132.
17. Arbiser JL, Raab G, Rohan RM, et al. (1999) Isolation of mouse stromal cells associated with a human tumor using differential diphtheria toxin sensitivity. *Am. J. Pathol.* **155**: 723–729.
18. Arbiser JL, Moses MA, Fernandez CA, et al. (1997) Oncogenic H-ras stimulates tumor angiogenesis by two distinct pathways. *Proc. Natl. Acad. Sci. USA* **94**: 861–866.
19. Gressani KM, Rollins LA, Leone-Kabler S, et al. (1998) Induction of mutations in Ki-ras and INK4a in liver tumors of mice exposed in utero to 3-methylcholanthrene. *Carcinogenesis* **19**: 1045–1052.
20. Gressani KM, Leone-Kabler S, O'Sullivan MG, et al. (1999) Strain-dependent lung tumor formation in mice transplacentally exposed to 3-methylcholanthrene and post-natally exposed to butylated hydroxytoluene. *Carcinogenesis* **20**: 2159–2165.
21. Rollins LA, Leone-Kabler S, O'Sullivan MG, Miller MS. (1998) Role of tumor suppressor genes in transplacental lung carcinogenesis. *Mol. Carcinog.* **21**: 177–184.
22. Zakut-Houri R, Oren M, Bienz B, et al. (1983) A single gene and a pseudogene for the cellular tumour antigen p53. *Nature* **306**: 594–597.
23. Hegi ME, Soderkvist P, Foley JF. (1993) Characterization of p53 mutations in methylene chloride-induced lung tumors from B6C3F1 mice [see comments]. *Carcinogenesis* **14**: 803–810.
24. Herman JG, Graff JR, Myohanen S, et al. (1996) Methylation-specific PCR: a novel PCR assay for methylation status of CpG islands. *Proc. Natl. Acad. Sci. USA* **93**: 9821–9826.
25. Swafford DS, Middleton SK, Palmisano WA, et al. (1997) Frequent aberrant methylation of p16INK4a in primary rat lung tumors. *Mol. Cell Biol.* **17**: 1366–1374.
26. Arbiser JL, Weiss SW, Arbiser ZK, et al. (2001) Differential expression of active mitogen-activated protein kinase in cutaneous endothelial neoplasms: Implications for biologic behavior and response to therapy. *J. Am. Acad. Dermatol.* **44**: 1–5.
27. Evans RM, Davies PJ, Costa M. (1982) Video time-lapse microscopy of phagocytosis and intracellular fate of crystalline nickel sulfide particles in cultured mammalian cells. *Cancer Res.* **42**: 2729–2735.
28. Bencko V. (1983) Nickel: a review of its occupational and environmental toxicology. *J. Hyg. Epidemiol. Microbiol. Immunol.* **27**: 237–247.
29. Huang X, Zhuang Z, Frenkel K. (1994) The role of nickel and nickel-mediated reactive oxygen species in the mechanism of nickel carcinogenesis. *Environ. Health Perspect.* **102** Suppl 3: 281–284.
30. Heinemann DE, Lohmann C, Siggelkow H. (2000) Human osteoblast-like cells phagocytose metal particles and express the macrophage marker CD68 in vitro. *J. Bone Joint Surg. Br.* **82**: 283–289.
31. Ben Izhak O, Vlodaysky E, Ofer A, et al. (1999) Epithelioid angiosarcoma associated with a Dacron vascular graft. *Am. J. Surg. Pathol.* **23**: 1418–1422.
32. Kirkpatrick CJ, Alves A, Kohler H, et al. (2000) Biomaterial-induced sarcoma: A novel model to study preneoplastic change. *Am. J. Pathol.* **156**: 1455–1467.
33. Liang R, Senturker S, Shi X, et al. (1999) Effects of Ni(II) and Cu(II) on DNA interaction with the N-terminal sequence of human protamine P2: enhancement of binding and mediation of oxidative DNA strand scission and base damage. *Carcinogenesis* **20**: 893–898.
34. Salnikow K, Gao M, Voitkun V, et al. (1994) Altered oxidative stress responses in nickel-resistant mammalian cells. *Cancer Res.* **54**: 6407–6412.
35. Zaman K, Ryu H, Hall D, et al. (1999) Protection from oxidative stress-induced apoptosis in cortical neuronal cultures by iron chelators is associated with enhanced DNA binding of hypoxia-inducible factor-1 and ATF-1/CREB and increased expression of glycolytic enzymes, p21(waf1/cip1), and erythropoietin. *J. Neurosci.* **19**: 9821–9830.
36. Salnikow K, Wang S, Costa M. (1997) Induction of activating transcription factor 1 by nickel and its role as a negative regulator of thrombospondin I gene expression. *Cancer Res.* **57**: 5060–5066.
37. Zatterale A, Kelly FJ, Korkina LG, et al. (1999) Oxidative stress in cancer prone genetic diseases: a review. *Ann. Ist. Super. Sanita* **35**: 205–209.
38. Bartsch H, Ohshima H, Pignatelli B, Calmels S. (1992) Endogenously formed N-nitroso compounds and nitrosating agents in human cancer etiology. *Pharmacogenetics* **2**: 272–277.
39. Mansour SJ, Matten WT, Hermann AS, et al. (1994) Transformation of mammalian cells by constitutively active MAP kinase. *Science* **265**: 966–970.
40. Cowley S, Paterson H, Kemp P, Marshall CJ. (1994) Activation of MAP kinase kinase is necessary and sufficient for PC12 differentiation and for transformation of NIH 3T3 cells. *Cell* **77**: 841–852.
41. Linardopoulos S, Street AJ, Quelle DE, et al. (1995) Deletion and altered regulation of p16^{ink4a} and p15^{INK4b} in undifferentiated mouse skin tumors. *Cancer Res.* **55**: 5168–5172.
42. Hussussian CJ, Struewing JP, Goldstein AM, et al. (1994) Germline p16 mutations in familial melanoma. *Nat. Genet.* **8**: 15–21.
43. Moskaluk CA, Hruban RH, Kern SE. (1997) p16 and K-ras gene mutations in the intraductal precursors of human pancreatic adenocarcinoma. *Cancer Res.* **57**: 2140–2143.
44. Cody DT, Huang Y, Darby CJ, et al. (1999) Differential DNA methylation of the p16 INK4A/CDKN2A promoter in human oral cancer cells and normal human oral keratinocytes. *Oral Oncol.* **35**: 516–522.
45. Wong AK, Chin L. (2000) An inducible melanoma model implicates a role for RAS in tumor maintenance and angiogenesis. *Cancer Metastasis Rev.* **19**: 121–129.
46. Klatfer R, Arbiser JL. (2000) Regulation of angiogenesis and tumorigenesis by signal transduction cascades: lessons from benign and malignant endothelial tumors. *J. Investig. Dermatol. Symp. Proc.* **5**: 79–82.
47. Tsao H, Zhang X, Fowlkes K, Haluska FG. (2000) Relative reciprocity of NRAS and PTEN/MMAC1 alterations in cutaneous melanoma cell lines. *Cancer Res.* **60**: 1800–1804.